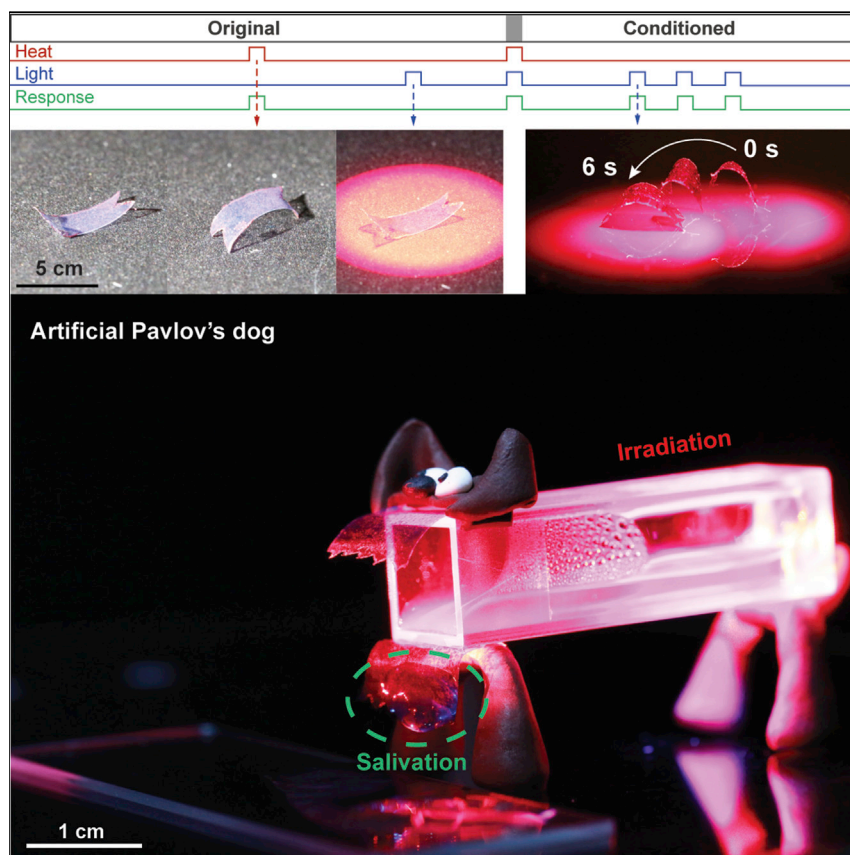


Article

Associative Learning by Classical Conditioning in Liquid Crystal Network Actuators



Aiming toward bioinspired materials whose responsivity evolves depending on their history, we disclose programmable liquid crystal polymer networks that “learn” to respond to an initially neutral stimulus (light) after association with an intrinsically effective stimulus (heating). The concept is inspired by the Pavlovian conditioning and enables soft robots that learn to walk, grippers that recognize different irradiation colors, and an artificial Pavlov’s dog. This is a step toward actuators that algorithmically mimic elementary aspects of learning.

Hao Zeng, Hang Zhang, Olli Ikkala, Arri Priimagi

olli.ikkala@aalto.fi (O.I.)
arri.priimagi@tuni.fi (A.P.)

HIGHLIGHTS

A synthetic material that emulates algorithmically associative learning is disclosed

The present material learns to respond to an initially neutral stimulus by bending

A soft thermoresponsive strip can be conditioned to walk upon irradiation

Gripping devices can be conditioned to differentiate irradiation colors

Zeng et al., *Matter* 2, 194–206
January 8, 2020 © 2019 The Author(s).
Published by Elsevier Inc.
<https://doi.org/10.1016/j.matt.2019.10.019>



Demonstrate

Proof-of-concept of performance with intended application/response



Article

Associative Learning by Classical Conditioning in Liquid Crystal Network Actuators

Hao Zeng,^{1,3} Hang Zhang,^{2,3} Olli Ikkala,^{2,*} and Arri Priimagi^{1,4,*}

SUMMARY

Responsive and shape-memory materials allow stimuli-driven switching between fixed states. However, their behavior remains unchanged under repeated stimuli exposure, i.e., their properties do not evolve. By contrast, biological materials allow learning in response to past experiences. Classical conditioning is an elementary form of associative learning, which inspires us to explore simplified routes even for inanimate materials to respond to new, initially neutral stimuli. Here, we demonstrate that soft actuators composed of thermoresponsive liquid crystal networks “learn” to respond to light upon a conditioning process where light is associated with heating. We apply the concept to soft microrobotics, demonstrating a locomotive system that “learns to walk” under periodic light stimulus, and gripping devices able to “recognize” irradiation colors. We anticipate that actuators that algorithmically emulate elementary aspects of associative learning and whose sensitivity to new stimuli can be conditioned depending on past experiences may provide new routes toward adaptive, autonomous soft microrobotics.

INTRODUCTION

Concepts from Stimuli-Responsive and Shape-Memory Materials to Associative Learning

Biological systems, viewed within the materials science perspective, are excessively complex. They involve reflexes and are adaptive, multifunctional, dissipative, self-regulating, and capable of evolving and learning from their past experiences. Nevertheless, biological systems have provided a great source of inspiration for scientists aiming to design functionalities for advanced materials.^{1–3} While bioinspired materials invariably require dramatic simplifications compared to their biological counterparts, sophisticated concepts to control, e.g., the mechanical properties, wetting characteristics, or structural colors, have been developed.^{1–3} On the other hand, a large variety of stimuli-responsive materials, whose properties can be reversibly switched between the original and activated states upon application and removal of an external stimulus, have been developed.^{4–7} They can also allow routes for functional bioinspired materials. Some stimuli-responsive systems exhibit shape morphing and locomotion,^{8,9} and autonomous soft robotic systems simplistically mimicking some aspects of biological responses have been devised.^{10,11} Out-of-equilibrium chemical and physical systems have also become prominent,^{12–22} suggesting new concepts for the design of dissipative bioinspired systems and devices. An evident route toward complex bioinspired functions would be to involve computer-code-based artificial intelligence to control the responses of material systems.²³ However, can one go beyond the examples presented thus far and develop

Progress and Potential

As described by Eric R. Kandel in his Nobel lecture, habituation, sensitization, and classical conditioning are the elementary forms of biological learning, which involves prohibitive complexity. Trying to capture even the slightest elements thereof in artificial materials is a grand challenge. We demonstrate soft actuators based on liquid crystal networks that show programmed associative learning behavior, inspired by the classical conditioning experiments on dogs. The thermoresponsive network evolves to respond to light upon conditioning, whereby the initially neutral light stimulus is applied together with heating. The conditioned actuator enables soft robotic devices that “learn” to translocate, or grippers that can be conditioned to differentiate irradiation colors. A modular artificial dog is also demonstrated that salivates upon a neutral stimulus. These findings suggest generalization from association of stimuli to soft systems that evolve depending on their history.



autonomous, adaptive artificial systems whose time-dependent behavior could evolve solely based on inherent material properties and the applied combinations of stimuli?

We propose that concepts inspired by the simplest forms of associative learning can act as a guide to design adaptive functional materials. Learning can be considered as a sequence of processes whereby a biological system or organism modifies its behavior upon past experiences.^{24,25} The mechanisms of learning are intractable in its full complexity, involving perception, memory, reflex, motor functions, mind, thought, consciousness, and reward-seeking, many of which have been connected solely to living organisms. Living organisms also show great flexibility in learning to respond to different stimuli, allowing in general widely different responses depending on their history. Still, by limiting to sufficiently simple organisms, more tractable forms of learning and adaptation are encountered, involving a restricted number of responses. In the reductionistic way described by Eric R. Kandel based on his studies on *Aplysia*, habituation, sensitization, and classical conditioning can be considered as the elementary forms of learning.²⁶ In the context of synthetic materials, behaviors inspired by classical conditioning have been implemented using electric^{27,28} or biochemical circuitry.^{29–31} Algorithmic programming of common inanimate materials to show even the most elementary aspects of learning is still a particularly imposing challenge.

We recently demonstrated an association process whereby a synthetic temperature-responsive hydrogel containing plasmonic gold nanoparticles and merocyanine-based photoacid became responsive to light, to which it was originally indifferent, to allow a new stimulus for gel melting.³² Algorithmically, the evolution in the material response was inspired by the classical conditioning process observed by Pavlov on dogs.²⁴ Dealing with two fixed stimuli and a response under carefully chosen conditions can be considered to correspond to some selected processes of simple animals with limited number of reflexes.²⁶ Inherent for the concept was to combine the two engineered stimuli responses with a memory concept, provided by chain-like self-assembly of gold nanoparticles.³²

Here, we suggest a different concept of associative learning involving soft actuators comprising liquid crystal polymer networks (LCNs), also using two stimuli (light and heat) but in this case based on a different memory concept: temperature-dependent diffusion kinetics of light-absorbing dyes into the LCN, leading to their rearrangement. As shown by the schematics in Figure 1A, the LCN initially responds to heat by bending (the intrinsic response, corresponding to the dog salivation for food) but not to light irradiation (corresponding to the bell that does not lead to the salivation). Upon the association process involving simultaneous exposure to light irradiation and heat, the LCN becomes light responsive, showing bending by exposure to light (corresponding to the bell leading to salivation after conditioning). As a result of the association process, the material properties can be conditioned to become responsive to a new stimulus. This characteristic distinguishes the present actuator from conventional responsive and shape-memory materials, whereby the stimuli for the allowed responses remain unchanged, as schematically illustrated in Figures 1B and 1C, respectively. To apply the concept to soft robotics, we present a locomotive structure that “learns” to walk upon periodic light irradiation and a gripping device that differentiates irradiation colors (in resemblance to tuning of the neutral stimulus), by association of light with heat. Finally, to demonstrate the modularity of the approach, we construct an artificial Pavlov’s dog by integrating the actuator with the gel³² implemented with an associative memory, both sharing the same stimuli.

¹Smart Photonic Materials, Faculty of Engineering and Natural Sciences, Tampere University, P.O. Box 541, 33101 Tampere, Finland

²Department of Applied Physics, Aalto University, P.O. Box 15100, 02150 Espoo, Finland

³These authors contributed equally

⁴Lead Contact

*Correspondence: olli.ikkala@aalto.fi (O.I.), arri.priimagi@tuni.fi (A.P.)

<https://doi.org/10.1016/j.matt.2019.10.019>

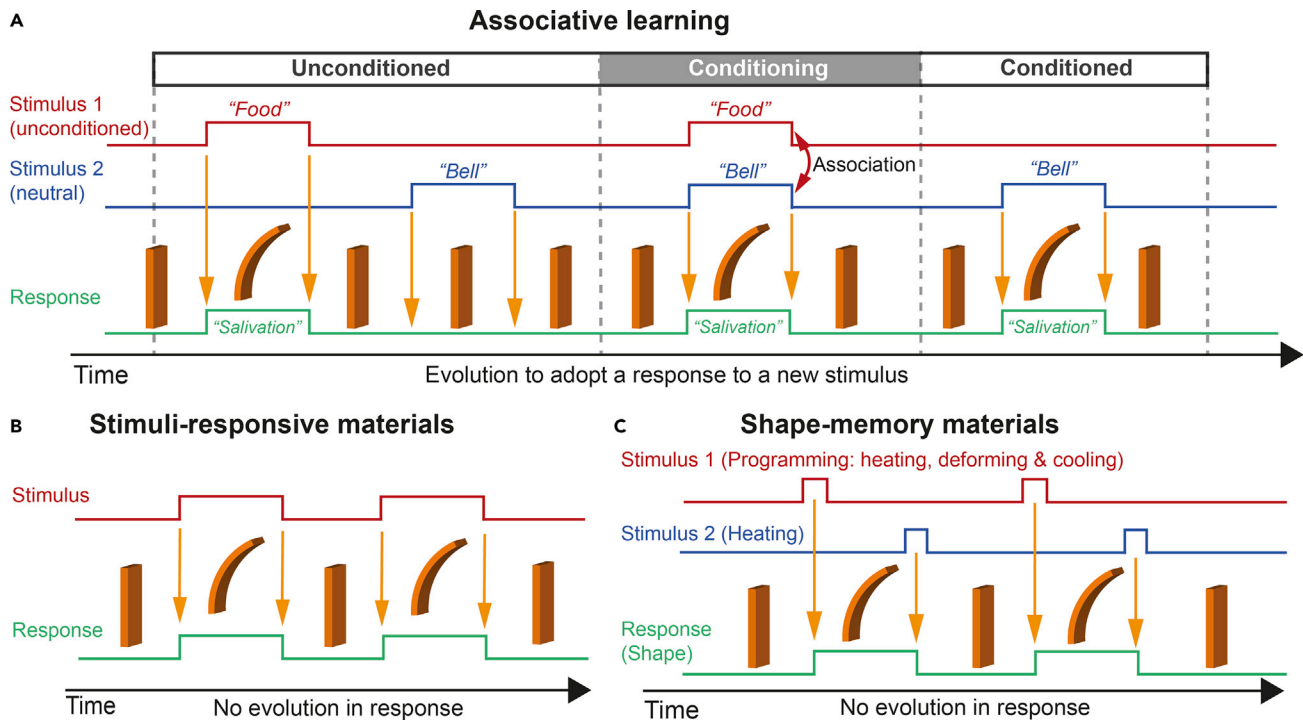


Figure 1. Schematics Showing the Distinction between Stimuli-Responsive and Shape-Memory Materials and Materials Allowing Associative Learning by Classical Conditioning, Illustrated by the Bending of an Originally Flat Film

(A) Programming inspired by classical conditioning allows the material to become responsive to an originally neutral stimulus upon associating two stimuli.

(B and C) The behaviors of stimuli-responsive materials (B) and shape-memory materials (C) remain unchanged in repeated exposures of stimuli, and do not evolve to become responsive to new, originally neutral, stimuli. This simplified scheme highlights only the most fundamental differences of the classical conditioning from stimuli-responsive and shape-memory materials. Therefore, for clarity, irreversible stimuli-responsive and shape-memory materials with several temporary states are not illustrated.

RESULTS

Actuator with an Associative Memory

In LCNs, the interplay between the thermal expansion of the material and control over mesogen orientation within the self-assembled network classically allows macroscopic actuation in response to a variety of external stimuli.^{33,34} Alignment programming enables the design of actuators with versatile deformation modes^{35,36} and externally controlled devices with sophisticated properties.^{37,38} Recently, reconfigurable actuators based on, for example, dynamic covalent bonds^{39,40} or synergistic use of photochemical and photothermal effects⁴¹ have been demonstrated to yield multiple deformation modes under identical illumination conditions, allowed by a programming step prior to the shape morphing. However, no actuators that can be activated by a new, initially neutral stimulus, to allow response upon conditioning, have been presented. The development of the LCN actuator with an associative memory (as opposed to other types of stimuli-responsive systems) is motivated by the following three reasons: (1) stimuli-driven actuation such as contraction or bending is reversible and easy to quantify, rendering changes in the material response straightforward to monitor; (2) LCNs are intrinsically thermoresponsive, and often sensitive also to other stimuli such as light, serving as a good basis for choosing the stimuli; (3) the field of soft robotics is drawing growing attention,^{42,43} and soft devices that “learn” could provide unforeseen opportunities for future microrobotics.

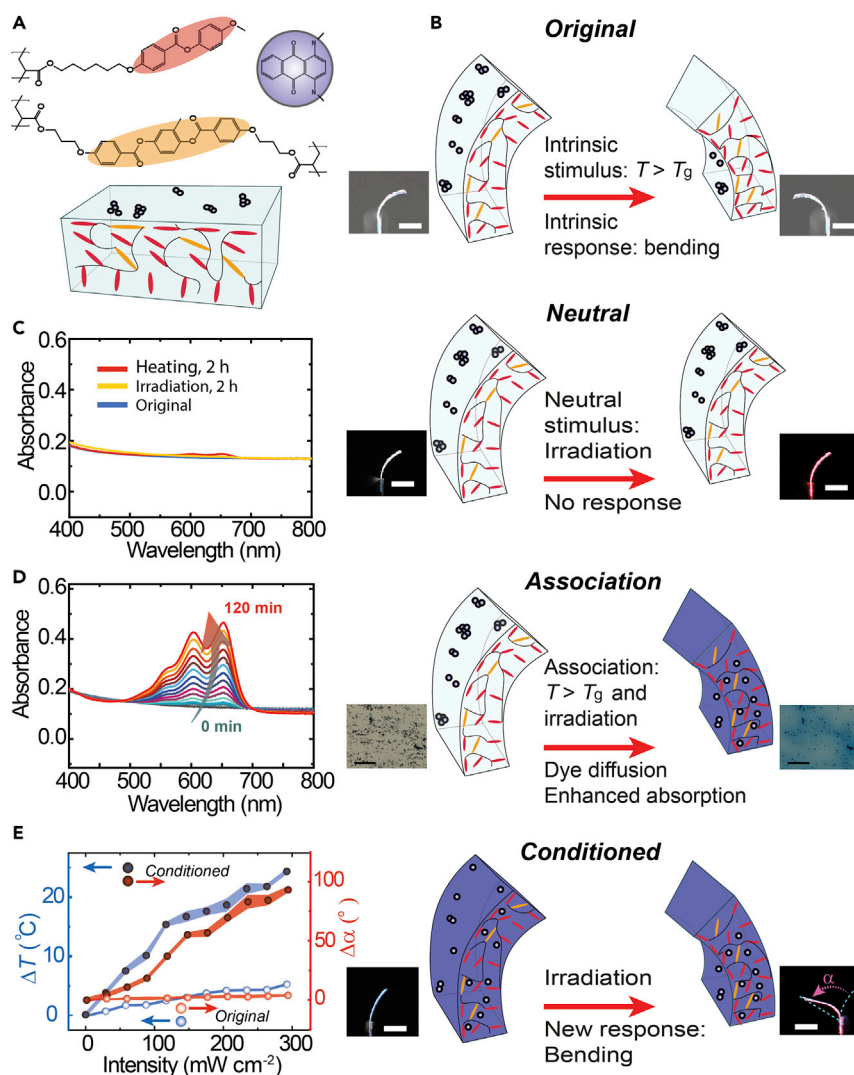


Figure 2. Classically Conditioned Actuator by Associating Two Stimuli

(A) The splay-aligned LCN actuator and the dye initially applied selectively on the planar-aligned surface.

(B) Bending of the actuator upon heating above T_g , illustrated schematically and by photographs. Scale bars, 2 mm.

(C) The original sample under neutral stimulus (irradiation at 635 nm, 300 mW cm^{-2}) showing no essential response. Left: UV-vis spectrum of the original actuator upon irradiation or heating at 70°C for 2 h. Scale bars, 2 mm.

(D) Association of heating and irradiation. Left: UV-vis spectra during simultaneous exposure to heat and light. Insets: optical micrographs of the surface before and after the association. Scale bars, 100 μm .

(E) Light response after association. Left: light-induced heating and deformation in “conditioned” and original samples. Error bars (indicated by the widths of the lines connecting the measured points) denote standard deviations for $n = 3$ measurements. Insets: photographs showing the response of the “conditioned” sample under irradiation and the bending angle (α). Scale bars, 2 mm.

The present actuator is based on a splay-aligned LCN film covered on the planar side with a dye, Disperse Blue 14 (Figure 2A), which acts as a light absorber. The splayed alignment ensures bending upon heating as the intrinsic (unconditioned) response, and heating can also be achieved via light absorption by the dyes and subsequent photothermal effects.¹⁰ The programmed response is shown in Figures 2B–2E. As

expected,⁴⁴ heating above the glass transition temperature ($T_g \approx 40^\circ\text{C}$, see [Figure S1](#)) leads to gradual bending toward the planar-oriented side of the film ([Figures 2B and S2](#)). Note that the LCN actuator shows an initial curvature toward the homeotropic side due to anisotropic thermal expansion during cooling from polymerization temperature to room temperature. Irradiation at 635 nm yields negligible bending ([Figure 2C](#)), as the dye particles are localized only at scattered spots on the surface, and most of the incident light (>80%) simply penetrates the sample or is scattered by the dye clusters. Therefore, the light absorbed by them is insufficient to induce bulk heating of the actuator. The moderate temperature enhancement is due to dyes being clustered on the surface, in combination with relatively low irradiation intensity ([Figure S3](#)). Light-induced heating of the bulk LCN is dictated by the dye distribution, while sample dimensions yielding different thermal gradient conditions also affect the achievable temperature. [Figures S4 and S5](#) present detailed photothermal characterization by infrared imaging.

The light response can be promoted by diffusion of the dye molecules into the interior polymer network, thus providing a time scale for the association process, i.e., time-dependent memory. Driven by heat, the dye molecules initially confined to random positions on the planar sample surface start diffusing into the bulk network, leading to an increase in the overall light absorption. The diffusion flux J is given by the Fick's law,⁴⁵ $J(T) = -D(T) \frac{d\phi}{dx}$, where D is the dye diffusivity at temperature T , ϕ the molar concentration of the dye, and $\frac{d\phi}{dx}$ the dye concentration gradient at the dye-polymer interface. [Figure S6](#) presents J at different temperatures, showing that the diffusion remains negligible up to 80°C but rapidly increases above 100°C . This explains the fact that upon heating to 70°C or irradiation (photothermal heating $<20^\circ\text{C}$; [Figures S3 and S4](#)), the dye diffusion is limited and the change in material absorption negligible ([Figure 2C](#)). More details on diffusion flux calculation are given in [Experimental Procedures](#).

[Figure 2D](#) shows the association process upon simultaneous exposure to heat and light. When the dyes diffuse into the bulk of the LCN film, the overall light absorption increases, which in turn boosts the photothermal effect and further raises the sample temperature. Under such self-enhancing conditions, the sample temperature rises above 120°C after simultaneous exposure to both stimuli for 1 h ([Figure S7](#)), resulting in a significant enhancement of light absorption due to efficient dye diffusion ([Figure S8](#)). The "conditioned" sample exhibits a clear spectral change ([Figure 2D](#) and sample photographs in [Figure S9](#)), therefore enabling significantly enhanced photothermal heating upon irradiation ([Figures 2E and S10](#)). The dye diffusion serves as the time constant and the dye rearrangement as a memory that associates the irradiation with the unconditioned stimulus ([Figure 2D](#)).

The actuator "learns" to respond to the irradiation by bending after the association process, as depicted by the thermal camera images shown in [Figure 3](#). Before the association, the strip exhibits negligible photoactuation, with about 4° bending and maximum 5°C temperature increase upon 290 mW cm^{-2} irradiation. The conditioning enables the material to evolve to a new state, in which the strip shows 25°C temperature increase and $>90^\circ$ bending under identical irradiation conditions. This corresponds to a 5-fold increase in the photogenerated heat and a 20-fold increase in the light-induced deformation as compared with the unconditioned sample ([Figure 2E](#)).

Soft Robots and Conditioning with Associative Memory

As shown above, the process inspired by classical conditioning enables a thermoresponsive material to "learn" to respond to light, i.e., to show the response (bending) based on an initially neutral stimulus (light). We believe, more generally, that acquiring

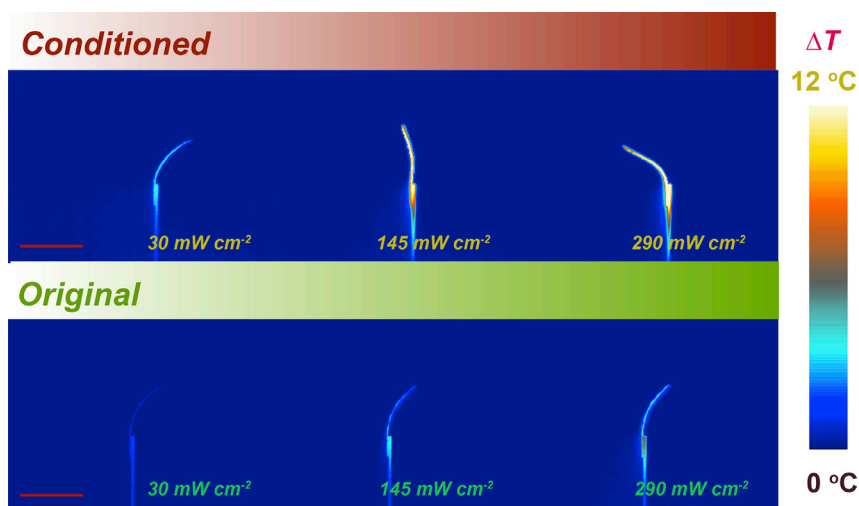


Figure 3. Thermal Camera Images for Light Actuation

Light-induced deformation and photothermal heat generation are significantly enhanced through the association process. The temperature scale is chosen such that it properly enhances the image contrast. The exact temperature increase is given in Figure 2E. Scale bars, 4 mm.

new stimuli for the responses by association processes becomes important for the emergent wireless soft microrobotics.^{46,47} Light is an attractive energy source for remotely controlled microrobotics due to its tunability (e.g., in wavelength and intensity) and the high degree of spatial and temporal control over the properties of light fields.^{48,49} Figures 4A–4E illustrate the role of the association process in devising a locomotive robot that “learns” to walk by irradiation. The LCN-based robot is initially sensitive to heat to allow bending and locomotion only by thermal pulses, but is insensitive to light (Figures 4A–4C), yet becomes light-active after associating the two stimuli (Figures 4D and 4E) through the mechanism explicated in Figure 2. Under temporally modulated irradiation, the “conditioned” soft robot starts to walk (velocity $\sim 1 \text{ mm s}^{-1}$) on a surface with asymmetric friction (Figures 4F and S11; Video S1), which is beyond its capabilities before the conditioning process.

Biologically, the classical conditioning can take place in response to a variety of stimuli, thus enabling the animal to adapt to different changes in environmental conditions.⁵⁰ For instance, the bell in the classical Pavlov’s dog experiment could be replaced by an arbitrary stimulus the dog can perceive, for example, music or a flash of light. While the diversity of applicable neutral stimuli in our present artificial materials is limited though expandable by using multicomponent hybrids, we next demonstrate some degree of tunability in its choice, more specifically the differentiation between light colors. The associative memory in the present actuator relies on the time constants given by the dye diffusion from one surface to the bulk, leading to their rearrangement, and, due to the wealth of dyes with different spectral properties available, the absorption region can be easily tuned. This tunability is exemplified in Figure S12 where dyes absorbing near-UV (Disperse Orange 3), blue-green (Disperse Red 1), and red light (Disperse Blue 14) are used for the association process upon 405, 488, and 635 nm irradiation, respectively. Utilizing the spectral selectivity, we designed soft grippers that are tuned to recognize and respond to different colors of light after the association. Figure 4G shows photos of the actuator described above based on Disperse Blue Blue 14 (I, unconditioned; II, conditioned), as well as the conditioned one based on Disperse Red 1 (III). The

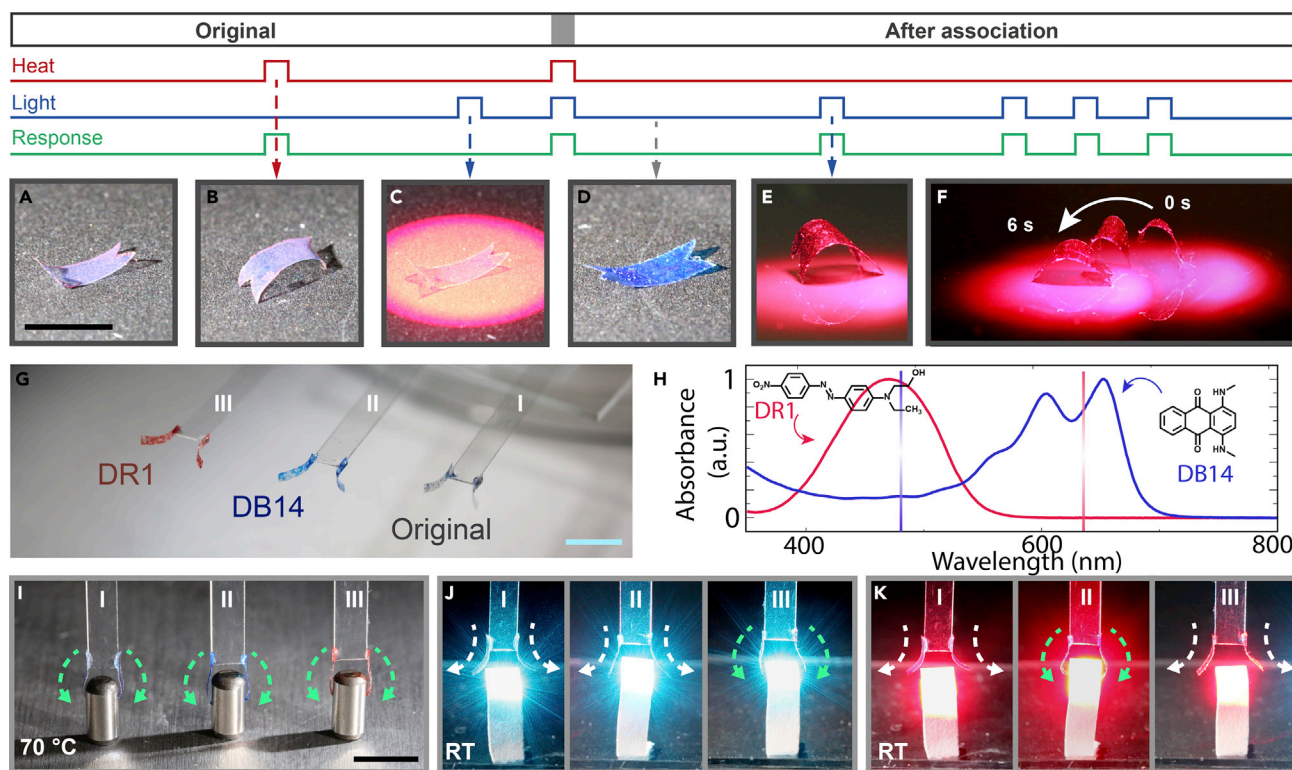


Figure 4. Pavlov-Inspired Soft Robots

(A–E) Training flow of the walker with associative memory. An original LCN-based walker (A) deforms upon heating (B) and is insensitive to light (C). After association of the two stimuli, the absorption of the walker around 635 nm increases (D), which allows for efficient photoactuation upon red-light irradiation (E).

(F) Superimposed images showing the “conditioned” walker translocating on a ratchet-structured surface under temporally modulated illumination.

(G–K) Grippers that learn to respond to different irradiation wavelengths. (G) Photographs of grippers composed of original actuator (I), associated with red light (II), and associated with blue light (III). (H) Chemical structures and absorption spectra of the dyes used and the wavelengths used for the association process. DR1, Disperse Red 1; DR14, Disperse Blue 14. (I) An original gripper (I) and grippers associated with red (II) and blue light (III) that close upon heating to 70°C. (J) Only gripper III closes upon irradiation with blue light (488 nm, 300 mW) that is scattered by the white paper strip at room temperature (RT). (K) Only gripper II closes upon irradiation with red light (635 nm, 300 mW) at RT. Dashed arrows indicate the opening (white) or closing (green) of the grippers. Scale bars, 5 mm.

spectra of the photosensitive dyes and the corresponding light wavelengths used for association process are shown in Figure 4H. All grippers are thermoresponsive, closing around an inserted object at sufficiently high temperature (Figure 4I). Once they are placed in front of a strongly scattering object (a white paper strip for demonstration), the “conditioned” grippers only close when the wavelength of the scattered light matches the absorption range of the dye (red light for gripper II, blue light for gripper III), while the original gripper remains indifferent to irradiation (Figures 4J and 4K). More details on the gripper realization and light actuation are presented in Figure S13.

Finally, we demonstrate the concept of materials with associative memory by constructing an artificial Pavlov’s dog, whereby the previously reported hydrogel³² serves as the reservoir of “saliva” and the LCN actuators function mechanically as the dog’s “jaws” (Figure 5A). As discussed in detail in Zhang et al.,³² the gel melts when heated above 33°C and also upon light irradiation (635 nm + 455 nm, $140 \pm 25 \text{ mW cm}^{-2}$) after associating light with heat. The gel and the actuator can be easily combined because they share the same stimuli (heat and light). For

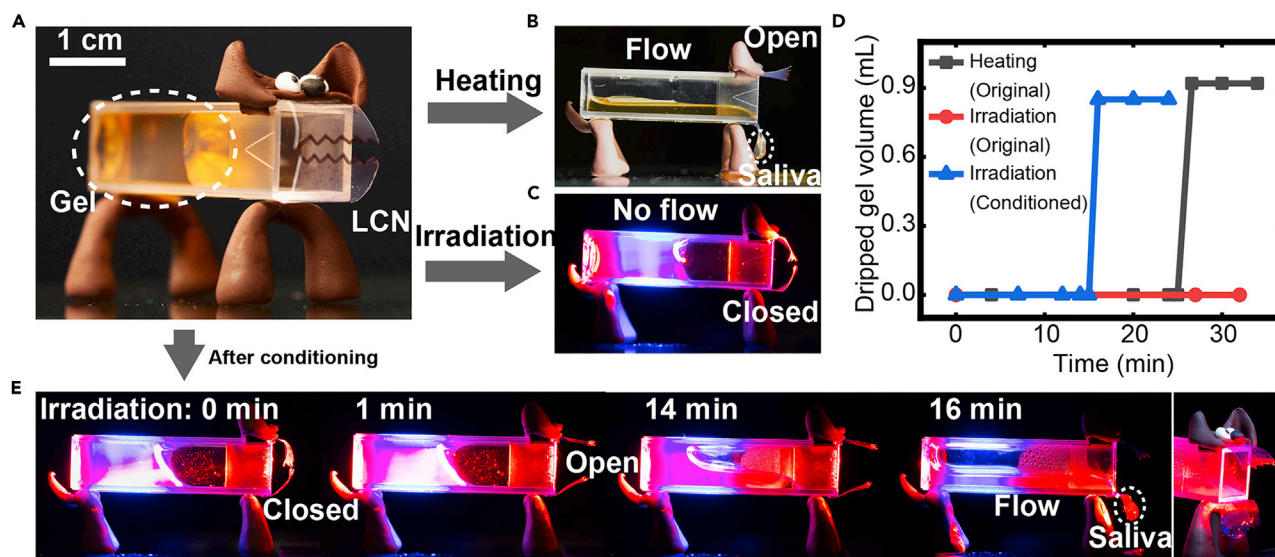


Figure 5. An Artificial Pavlov's Dog

(A) Photographs of the original dog assembled from a cuvette containing Pavlov-inspired gel (saliva) and LCN jaws.

(B) Side view of the original dog after incubation at 50°C for 27 min, showing salivation (gel dripping).

(C) The original artificial dog after irradiation for 27 min, yielding no response.

(D) Volume of dripped gel in original and “conditioned” dog.

(E) The salivation process upon light irradiation (635 nm, 300 mW cm⁻²) after association. The last image highlights the head after salivation. The irradiation consists of 635 nm (300 mW cm⁻²) laser on the whole dog and 455 nm light (25 mW cm⁻²) on the gel part.

Scale bar, 1 cm.

the original dog, heating (“food”) leads to opening of the jaws and simultaneous melting of the gel, which flows out of the cuvette and mimics salivation (Figure 5B). The jaws opened in a few minutes, while the “saliva” started to drip out from the mouth in 26 min, after initial accumulation due to surface tension of the liquid (Figures 5D and S14). Upon irradiation (“bell”), the jaws of the original dog remained closed and no gel melting was observed (Figure 5C). After the association process, the dog responded to irradiation by opening its jaws and salivating (Figure 5E). Here the induction time for salivation is shorter than upon external heating, which originates from the faster temperature increase within the gel by photothermal heating. In this way, an artificial Pavlov's dog was constructed that could modify its behavior as a result of previous experience, demonstrating the possibility of constructing a modular, artificial system that algorithmically mimics a simplistic learning process.

DISCUSSION

It is important to highlight that conceptually, the actuator with an associative memory differs from conventional responsive or shape-memory materials^{6,51–53} and from reconfigurable actuators.^{39–41} Conventional stimuli-responsive materials respond to an imposed stimulus, such as temperature, pH, or external fields (Figure 1B).⁶ The response can be highly sophisticated or driven by several fixed stimuli, but the materials do not evolve—they do not allow any new stimuli to trigger the original response. On the other hand, shape-memory materials involve temporary states produced, for example, by heating, mechanical deformation, and subsequent cooling, followed by recovery of the original state upon heating (Figure 1C).⁵¹ A large variety of shape-memory materials using different stimuli and temporary states has been developed.^{52,53} However, they do not evolve to provide the original response upon imposing a new, initially neutral stimulus.

Reconfigurable LCN actuators have recently attained increasing attention.^{39–41,54–57} Conventional implementation strategy typically adopts a programming step during fabrication in order to obtain customized forms of actuation in different samples or different segments within a single sample.⁵⁸ The concept of reconfigurability allows reprogramming after the fabrication process, allowing one single structure to perform multiple shape changes (responses) upon one identical stimulus. Thus, the reprogrammability conceptually differs from the associative learning and classical conditioning, whereby the original response is achieved by a new stimulus upon the conditioning.

Compared with biological systems exhibiting complex responses to stimuli and ability to adapt to various stimuli, admittedly the materials demonstrated here are highly simplistic and prescribed to preselected types of stimuli. The stimuli used in the original Pavlovian conditioning are fully orthogonal, the food providing a visual signal and the bell causing an auditory response. Both pathways involve complex physiological processes, and are finally associated in the brain to trigger the memory (salivation) after conditioning. In the present actuator system, however, light stimulus is an effector intrinsically equivalent to heating: it is absorbed and transformed into heat to trigger the deformation. The dye diffusion process (the memory) is temperature dependent, and heat and light (photothermal heating) contribute through the same pathway. Therefore, at sufficiently high temperature, heating alone also induces strong dye diffusion and the corresponding enhancement of bulk absorption (Figure S6). Similarly, light irradiation with sufficiently high intensity ($>2 \text{ W cm}^{-2}$) can give rise to bending deformation without the association process (Figure S15). As shown in Figure S6, above the temperature of ca. 80°C , the dyes start to diffuse from surface into the bulk to form the memory. Therefore, to algorithmically mimic the conditioning process, the system parameters, such as irradiation intensity and conditioning temperature, must be carefully tuned within a suitable range (Figure S16). Within this parameter range, associative learning can be algorithmically but not mechanically mimicked, even if in a dramatically simplified manner. We note that also many artificial biochemical systems showing associative learning behavior require optimization,^{28,30} and that physical limits (e.g., stimuli strength, application time) also exist in biological systems.²⁴ Even if still limited, we envision that the concept proposed can be generalized to other types of soft matter systems and other stimuli, to exhibit even more sophisticated processes to evolve in material behavior.

A further step toward mimicking psychological behaviors in synthetic materials could be to mimic the forgetting process. However, due to the irreversibility of entropy-driven dye diffusion, extinction of the “learned” response is challenging. Potential approaches could include the use of absorbing molecules or particles with dynamic properties,³² responsive-material-based logic gates, or more complex intelligent responses.⁵⁹ In Figure S17, we show that it is possible to externally manipulate the artificial memory using chemicals. The absorbance of a conditioned sample drops by 80% by bathing in isopropanol for 15 min at 70°C . Note that this process only mimics the apparent forgetting-like behavior using chemical compounds and significantly differs from its biological counterpart, in which no chemical additives are required to drive the forgetting.

Conclusions

We have designed a stimuli-driven actuator based on LCNs whose response is inspired by classical conditioning, one of the elementary forms of learning. The actuator “learns” to respond to an initially neutral stimulus (light) through an association

process, which connects neutral stimulus (light) with an intrinsic stimulus (heat). Concrete potential for soft robotic applications is demonstrated by devising a walker and color-recognizing grippers that evolve to respond to light upon the association process, and modularity of the concept is further highlighted, curiously, by constructing an artificial Pavlov's dog. We believe that the dynamic responses and programmability of the actuators, together with the diversity in their responsiveness to stimuli, may provide unforeseen routes toward soft microrobotics that can self-adapt and learn.

EXPERIMENTAL PROCEDURES

Materials

For the LCN, the light-absorbing dyes (Disperse Blue 14, Disperse Red 1, Disperse Orange 3) and the photoinitiator (2,2-dimethoxy-2-phenylacetophenone, 99%) were purchased from Sigma-Aldrich. 4-Methoxybenzoic acid 4-(6-acryloyloxyhexyloxy) phenyl ester (LC monomer) and 1,4-bis-[4-(3-Acryloyloxypropyloxy)benzoyloxy]-2-methylbenzene (LC crosslinker) were purchased from Synthron Chemicals. For the synthesis of the Pavlov-inspired hydrogel, please refer to Zhang et al.³²

Preparation of the LCN-Dye Actuator

The LCN actuator was photopolymerized from a mixture consisting of 79 mol % of the LC monomer, 20 mol % of the LC crosslinker, and 1 mol % of the photoinitiator. The mixture was photopolymerized within a cell geometry made of two glass slides separated with 30- μm spacers (Thermo Scientific). The two glass slides were spin coated with 1 wt % water solution of polyvinyl alcohol (PVA, Sigma-Aldrich; 4000 rpm, 1 min) and homeotropic alignment layer (JSR OPTMER, 6000 rpm, 1 min), respectively. The PVA-coated glass surface was rubbed unidirectionally by using a satin cloth, and subsequently blown with high-pressure air to remove dust particles from the surface. The glass slides were glued together using UV-curable glue (UVS 91; Norland Products, Cranbury, NJ) to form the cell. The monomer mixture was prepared by magnetically stirring at 80°C (100 rpm) for 30 min. The mixture was then infiltrated into the cell using capillary force on a heating stage at 70°C and cooled down to 55°C at a rate of 5°C min⁻¹ to reach the nematic phase in a splay-aligned orientation. A UV light-emitting diode (Thorlabs; 20 mW cm⁻², 375 nm, 10 min) was used to polymerize the LC mixture at 55°C. Thereafter, the cell was opened and the LCN film was detached from the substrate by using a blade. Dye powder was spread uniformly on the surface involving the mesogen planar alignment using an optical cleaning tissue (Thorlabs). The LCN film was softened on a hot plate set at 70°C, then the dyed tissue was pressed on the top and the dye particles transferred to the LCN surface. Strip-like LCN was cut out from the sample film by using a blade, with the long axis matching the rubbing direction.

LCN Actuation, Association, and Characterization

Heat-triggered LCN actuation was carried out inside an oven with a cooling/heating rate of 0.2°C min⁻¹. Irradiation-induced bending was done by using a 635-nm laser source (Roithner Lasertechnik) with intensity up to 300 mW cm⁻². The heat-driven dye diffusion was carried out at 70°C on a hot plate for 5, 10, 20, 30, 50, 80, and 120 min. A piece of paper was placed between the hot-plate surface and the LCN film to reduce the adhesion of the LCN due to material softening at elevated temperatures. A microscope cover slide was placed on top of the LCN to maintain the flat shape. The light-driven diffusion was performed at room temperature, under 300 mW cm⁻² irradiation for the same time periods as listed above, whereby the laser was illuminated from the direction of the LCN top surface covered with dye particles. The association process, i.e., simultaneous heating and irradiation, was carried out at 70°C on a hot plate under an identical illumination condition (300 mW cm⁻²,

635 nm) for time periods of 5, 10, 20, 30, 40, 50, 60, 70, 80, 90, 100, 110, and 120 min. The temperature increase of the LCN film was measured with an infrared camera (FLIR, T420BX). The absorption spectra were measured with a UV-visible (UV-vis) spectrophotometer (Cary 60 UV-Vis, Agilent Technologies). Photographs were taken and movies recorded by using a Canon 5D Mark III camera. The dye-particle distribution and diffusion were quantified under an optical microscope (Zeiss Axio A1). The surface coverage of the dyes on the LCN surface was analyzed using ImageJ. Differential scanning calorimetry measurement was performed with a Mettler Toledo Star DSC821e instrument, using heating/cooling speeds of $10^{\circ}\text{C min}^{-1}$.

Diffusion Flux Measurement in LCN

Twenty microliters of Disperse Blue 14 (DB14) ethanol solution (10 mg in 1 mL, oversaturated) was dropped on the surface of an LCN film (30 μm). The dye covered the film surface homogeneously after evaporating the solvent. Thermal diffusion was carried out by setting different films (covered by dyes) on a hot plate at 50°C , 70°C , 90°C , 110°C , 120°C , and 130°C for different periods (1, 2, and 3 min). After each diffusion process, two baths of ethanol with sonication (10 s) were used to remove the remaining dyes on the film surface, and absorption spectra were measured (Figures S6A–S6F). According to Beer's law, the absorbance is given by $A = \epsilon l \frac{\rho c_m}{M_{\text{dye}}}$, where ϵ is the molar extinction coefficient, l is the sample thickness (30 μm), ρ is the material density (1.12 g cm^{-3}), c_m is the weight concentration of the dye, and M_{dye} is the molar mass of DB14 (266.3 g mol^{-1}). Based on absorbance of an LCN sample containing 0.32 wt % of DB14, we estimate ϵ to be about $1.6 \times 10^4 \text{ M}^{-1} \cdot \text{cm}^{-1}$, and the absorption cross-section, $\sigma = \epsilon/N_A$, to be $2.7 \times 10^{-17} \text{ cm}^2$ (where N_A is Avogadro's constant). The number of dye molecules n diffused into the LCN film per unit area in a period of time t can be calculated by $n = A \cdot \epsilon^{-1}$, and the diffusion flux $J = n \cdot t^{-1}$, as shown in Figures S6G and S6H.

Fabrication of the Artificial Pavlov's Dog

The artificial Pavlov's dog was constructed by a 3-mL disposable cuvette containing 2 mL of the Pavlov-inspired hydrogel to mimic the saliva and two pieces of the LCN film attached at the open end of the cuvette, to mimic the jaws. The association of the gel was done in a water bath at 50°C under 635 nm (140 mW cm^{-2}) + 455 nm (25 mW cm^{-2}) irradiation. The cuvette was then sealed with parafilm and stored in a fridge (4°C) overnight for gelation. The dog's face and feet were made from oven-hardening modeling clay (FIMO, Staedtler). The feet were designed so that the cuvette has a small tilting angle of $\sim 2^{\circ}$ to facilitate the flow of liquid. The gel and the LCN films were conditioned separately and reassembled for the "conditioned" dog. The heating experiment was carried out in a pre-heated oven (Vacu-therm, Heraeus) at 50°C , and the irradiation was done under 635 nm (300 mW cm^{-2}) laser illumination on the whole dog and 455 nm (25 mW cm^{-2}) only on the gel part. The volume of the gel dripped from the mouth was estimated from the remaining volume inside the cuvette.

SUPPLEMENTAL INFORMATION

Supplemental Information can be found online at <https://doi.org/10.1016/j.matt.2019.10.019>.

ACKNOWLEDGMENTS

The work is supported by the European Research Council (advanced grant DRIVEN, agreement no. 742829; starting grant PHOTOTUNE, agreement no. 679646), the Academy of Finland (Center of Excellence HYBER and competitive funding to

strengthen university research profiles no. 301820, the Flagship Program on Photonics Research and Innovation, PREIN, no. 320165, and a postdoctoral grant, nos. 316416 and 326445). We thank Dr. Terttu Hukka for assistance with differential scanning calorimetry, Markus Lahikainen for the help with UV-vis, Dr. Emilie Ressouche for the help with fabrication of the artificial dog, and Prof. Jaakko Timonen, Prof. Françoise Winnik, Prof. Petri Ala-Laurila, and Prof. André Gröschel for their valuable comments on the initial version of the manuscript. We also acknowledge the provision of facilities and technical support by Aalto University at OtaNano - Nanomicroscopy Center (Aalto-NMC).

AUTHOR CONTRIBUTIONS

A.P. and O.I. conceived and supervised the project. H. Zeng designed and fabricated the Pavlovian actuator. H. Zhang designed and fabricated the Pavlovian hydrogel. H. Zeng and H. Zhang carried out the experiments. All authors contributed to writing and revising the manuscript.

DECLARATION OF INTERESTS

The authors declare no competing interests.

Received: August 5, 2019

Revised: September 23, 2019

Accepted: October 25, 2019

Published: December 4, 2019

REFERENCES

- Bhushan, B. (2009). Biomimetics: lessons from nature—an overview. *Philos. Trans. R. Soc. A. Math. Phys. Eng. Sci.* 367, 1445–1486.
- Aizenberg, J., and Fratzl, P. (2009). Biological and biomimetic materials. *Adv. Mater.* 21, 387–388.
- Wegst, U.G.K., Bai, H., Saiz, E., Tomsia, A.P., and Ritchie, R.O. (2015). Bioinspired structural materials. *Nat. Mater.* 14, 23–36.
- Okano, T. (1998). *Biorelated Polymers and Gels* (Academic Press).
- Urban, M. (2011). *Handbook of Stimuli-Responsive Materials* (WILEY-VCH Verlag).
- Cohen Stuart, M.A., Huck, W.T., Genzer, J., Müller, M., Ober, C., Stamm, M., Sukhorukov, G.B., Szleifer, I., Tsukruk, V.V., Urban, M., et al. (2010). Emerging applications of stimuli-responsive polymer materials. *Nat. Mater.* 9, 101–113.
- Montero de Espinosa, L., Meesorn, W., Moatsou, D., and Weder, C. (2017). Bioinspired polymer systems with stimuli-responsive mechanical properties. *Chem. Rev.* 117, 12851–12892.
- Hines, L., Petersen, K., Lum, G.Z., and Sitti, M. (2017). Soft actuators for small-scale robotics. *Adv. Mater.* 29, 1603483.
- Palagi, S., and Fischer, P. (2018). Bioinspired microrobots. *Nat. Rev. Mater.* 3, 113–124.
- Wani, O.M., Zeng, H., and Priimagi, A. (2017). A light-driven artificial flytrap. *Nat. Commun.* 8, 15546.
- Wehner, M., Truby, R.L., Fitzgerald, D.J., Mosadegh, B., Whitesides, G.M., Lewis, J.A., and Wood, R.J. (2016). An integrated design and fabrication strategy for entirely soft, autonomous robots. *Nature* 536, 451–455.
- Grzybowski, B.A., Stone, H.A., and Whitesides, G.M. (2000). Dynamic self-assembly of magnetized, millimetre-sized objects rotating at a liquid-air interface. *Nature* 405, 1033–1036.
- Timonen, J.V.I., Latikka, M., Leibler, L., Ras, R.H.A., and Ikkala, O. (2013). Switchable static and dynamic self-assembly of magnetic droplets on superhydrophobic surfaces. *Science* 341, 253–257.
- Boekhoven, J., Hendriksen, W.E., Koper, G.J.M., Eelkema, R., and van Esch, J.H. (2015). Transient assembly of active materials fueled by a chemical reaction. *Science* 349, 1075–1079.
- Gerling, T., Wagenbauer, K.F., Neuner, A.M., and Dietz, H. (2015). Dynamic DNA devices and assemblies formed by shape-complementary, non-base pairing 3D components. *Science* 347, 1446–1452.
- Grzybowski, B.A., and Huck, W.T.S. (2016). The nanotechnology of life-inspired systems. *Nat. Nanotechnol.* 11, 585–592.
- Nijemeisland, M., Abdelmohsen, L.K.E.A., Huck, W.T.S., Wilson, D.A., and van Hest, J.C.M.A. (2016). Compartmentalized out-of-equilibrium enzymatic reaction network for sustained autonomous movement. *ACS Cent. Sci.* 2, 843–849.
- Merindol, R., and Walther, A. (2017). Materials learning from life: concepts for active, adaptive and autonomous molecular systems. *Chem. Soc. Rev.* 46, 5588–5619.
- Ashkenasy, G., Hermans, T.M., Otto, S., and Taylor, A.F. (2017). Systems chemistry. *Chem. Soc. Rev.* 46, 2543–2554.
- Sawczyk, M., and Klajn, R. (2017). Out-of-equilibrium aggregates and coatings during seeded growth of metallic nanoparticles. *J. Am. Chem. Soc.* 139, 17973–17978.
- van Esch, J.H., Klajn, R., and Otto, S. (2017). Chemical systems out of equilibrium. *Chem. Soc. Rev.* 46, 5474–5475.
- Che, H., Cao, S., and van Hest, J.C.M. (2018). Feedback-induced temporal control of “breathing” polymersomes to create self-adaptive nanoreactors. *J. Am. Chem. Soc.* 140, 5356–5359.
- Jordan, M.I., and Mitchell, T.M. (2015). Machine learning: trends, perspectives, and prospects. *Science* 349, 255–260.
- Pavlov, I.P. (1927). *Conditioned Reflexes* (Oxford Univ. Press).
- Pearce, J.M., and Bouton, M.E. (2011). Theories of associative learning in animals. *Annu. Rev. Psychol.* 62, 111–139.
- Kandel, E.R. (2006). *In Search of Memory: The Emergence of a New Science of Mind*, First Edition (W. W. Norton & Company).
- Jo, S.H., Chang, T., Ebong, I., Bhadviya, B.B., Mazumder, P., and Lu, W. (2010). Nanoscale

- memristor device as synapse in neuromorphic systems. *Nano Lett.* 10, 1297–1301.
28. Wu, C., Kim, T.W., Guo, T., Li, F., Lee, D.U., and Yang, J.J. (2017). Mimicking classical conditioning based on a single flexible memristor. *Adv. Mater.* 29, 1602890.
29. Ausländer, S., Ausländer, D., Müller, M., Wieland, M., and Fussenegger, M. (2012). Programmable single-cell mammalian biocomputers. *Nature* 487, 123–127.
30. MacVittie, K., Halánek, J., Privman, V., and Katz, E. (2013). A bioinspired associative memory system based on enzymatic cascades. *Chem. Commun.* 49, 6962–6964.
31. Zhang, H., Lin, M., Shi, H., Ji, W., Huang, L., Zhang, X., Shen, S., Gao, R., Wu, S., Tian, C., et al. (2014). Programming a Pavlovian-like conditioning circuit in *Escherichia coli*. *Nat. Commun.* 5, 3102.
32. Zhang, H., Zeng, H., Priimagi, A., and Ikkala, O. (2019). Programmable responsive hydrogels inspired by classical conditioning algorithm. *Nat. Commun.* 10, 3267.
33. Ikeda, T., Mamiya, J., and Yu, Y. (2007). Photomechanics of liquid-crystalline elastomers and other polymers. *Angew. Chem. Int. Ed.* 46, 506–528.
34. Ohm, C., Brehmer, M., and Zentel, R. (2010). Liquid crystalline elastomers as actuators and sensors. *Adv. Mater.* 22, 3366–3387.
35. White, T.J., and Broer, D.J. (2015). Programmable and adaptive mechanics with liquid crystal polymer networks and elastomers. *Nat. Mater.* 14, 1087–1098.
36. Ware, T.H., McConney, M.E., Wie, J.J., Tondiglia, V.P., and White, T.J. (2015). Voxellated liquid crystal elastomers. *Science* 347, 982–984.
37. Yamada, M., Kondo, M., Miyasato, R., Naka, Y., Mamiya, J.-i., Kinoshita, M., Shishido, A., Yu, Y., Barrett, C.J., and Ikeda, T. (2009). Photomobile polymer materials—various three-dimensional movements. *J. Mater. Chem.* 19, 60–62.
38. Zeng, H., Wani, O.M., Wasylczyk, P., Kaczmarek, R., and Priimagi, A. (2017). Self-regulating iris based on light-actuated liquid crystal elastomer. *Adv. Mater.* 29, 1701814.
39. Pei, Z., Yang, Y., Chen, Q., Terentjev, E.M., Wei, Y., and Ji, Y. (2014). Mouldable liquid-crystalline elastomer actuators with exchangeable covalent bonds. *Nat. Mater.* 13, 36–41.
40. Wang, Z., Tian, H., He, Q., and Cai, S. (2017). Reprogrammable, reprocessable, and self-healable liquid crystal elastomer with exchangeable disulfide bonds. *ACS Appl. Mater. Interfaces* 9, 33119–33128.
41. Lahikainen, M., Zeng, H., and Priimagi, A. (2018). Reconfigurable photoactuator through synergistic use of photochemical and photothermal effects. *Nat. Commun.* 9, 4148.
42. Whitesides, G.M. (2018). Soft robotics. *Angew. Chem. Int. Ed.* 57, 4258–4273.
43. Zeng, H., Wasylczyk, P., Wiersma, D.S., and Priimagi, A. (2018). Light robots: bridging the gap between microrobotics and photomechanics in soft materials. *Adv. Mater.* 30, 1703554.
44. Mol, G.N., Harris, K.D., Bastiaansen, C.W.M., and Broer, D.J. (2005). Thermo-mechanical responses of liquid-crystal networks with a splayed molecular organization. *Adv. Funct. Mater.* 15, 1155–1159.
45. Fick, A. (1995). On liquid diffusion. *J. Membr. Sci.* 100, 33–38.
46. Hu, W., Lum, G.Z., Mastrangeli, M., and Sitti, M. (2018). Small-scale soft-bodied robot with multimodal locomotion. *Nature* 554, 81–85.
47. Kohlmeyer, R.R., and Chen, J. (2013). Wavelength-selective, IR light-driven hinges based on liquid crystalline elastomer composites. *Angew. Chem. Int. Ed.* 52, 9234–9237.
48. Palagi, S., Mark, A.G., Reigh, S.Y., Melde, K., Qiu, T., Zeng, H., Parmeggiani, C., Martella, D., Sanchez-Castillo, A., Kapernaum, N., et al. (2016). Structured light enables biomimetic swimming and versatile locomotion of photoresponsive soft microrobots. *Nat. Mater.* 15, 647–654.
49. Rogó, M., Zeng, H., Xuan, C., Wiersma, D.S., and Wasylczyk, P. (2016). Light-driven soft robot mimics caterpillar locomotion in natural scale. *Adv. Opt. Mater.* 4, 1689–1694.
50. Holland, J.H. (1992). *Adaptation in Natural and Artificial Systems* (MIT Press).
51. Otsuka, K., and Ren, X. (2005). Physical metallurgy of Ti-Ni-based shape memory alloys. *Prog. Mater. Sci.* 50, 511–678.
52. Lendlein, A., Jiang, H., Jünger, O., and Langer, R. (2005). Light-induced shape-memory polymers. *Nature* 434, 879–882.
53. Lee, K.M., Koerner, H., Vaia, R.A., Bunning, T.J., and White, T.J. (2011). Light-activated shape memory of glassy, azobenzene liquid crystalline polymer networks. *Soft Matter* 7, 4318–4324.
54. Qian, X., Chen, Q., Yang, Y., Xu, Y., Li, Z., Wang, Z., Wu, Y., Wei, Y., and Ji, Y. (2018). Untethered recyclable tubular actuators with versatile locomotion for soft continuum robots. *Adv. Mater.* 30, 1801103.
55. Gelebart, A.H., Mulder, D.J., Vantomme, G., Schenning, A.P.H.J., and Broer, D.J. (2017). A rewritable, reprogrammable, dual light-responsive polymer actuator. *Angew. Chem. Int. Ed.* 56, 13436–13439.
56. Jiang, Z.C., Xiao, Y.Y., Tong, X., and Zhao, Y. (2019). Selective decrosslinking in liquid crystal polymer actuator for optical reconfiguration of origami and light-fueled locomotion. *Angew. Chem. Int. Ed.* 58, 5332–5337.
57. Ube, T., Kawasaki, K., and Ikeda, T. (2016). Photomobile liquid-crystalline elastomers with rearrangeable networks. *Adv. Mater.* 28, 8212–8217.
58. Yang, R., and Zhao, Y. (2017). Non-uniform optical inscription of actuation domains in a liquid crystal polymer of uniaxial orientation: an approach to complex and programmable shape changes. *Angew. Chem. Int. Ed.* 129, 14390–14394.
59. Lan, R., Sun, J., Shen, C., Huang, R., Zhang, L., Yang, H., et al. (2019). Reversibly and irreversibly humidity-responsive motion of liquid crystalline network gated by SO₂ gas. *Adv. Funct. Mater.* 29, 1900013.